Coupling issues in monthly forecasting

Frédéric Vitart

European Centre for Medium-Range Weather Forecasts
Reading, U.K.
Frederic.Vitart@ecmwf.int

1. Introduction

The European Centre for Medium-Range Forecasts (ECMWF) produces operational monthly forecasts since 2004 to fill the gap between medium-range weather forecasting and seasonal forecasting. In the present configuration, the atmospheric component (IFS) is forced by persisted SST anomalies during the first 10 days of integrations and is coupled to an OGCM after day 10.

The goal of the present paper is to discuss if the current configuration of the OGCM, which is coupled to the atmospheric model after day 10, is suitable for monthly forecasting. This OGCM has the same configuration as the OGCM used in seasonal forecasting system 3 (Anderson et al, 2007). This configuration has been designed mostly for the prediction of ENSO. This means that this oceanic model is capable of resolving ocean large scale dynamics, but the processes in the oceanic mixed-layer are poorly represented, because of the low vertical resolution in the upper ocean.

In the present paper, the skill of two different configurations of the monthly forecasting system is compared. In the first configuration, IFS is coupled to the OGCM used in operation. In the second configuration, IFS is coupled to an ocean mixed-layer model instead of an OGCM. The first configuration has a good representation of ocean dynamics, but a poor representation of the processes in the oceanic mixed layer. The second configuration does not simulate ocean dynamics, but has a good representation of the processes in the ocean mixed layer. Comparing those two configurations will give us an insight about which of those two processes (ocean dynamics or mixing processes) is more important for monthly forecasting. The answer is not necessarily obvious since the monthly time range may be long enough for the ocean dynamics to play an important role, through the evolution of SST anomalies associated to ENSO or the Indian Ocean dipole.

Section 2 will describe the current configuration of the ECMWF monthly forecasting system. Section 3 will describe the two experiments. In Section 4, the skill of the two configurations to predict a Madden Julian Oscillation (MJO) event will be discussed. Section 5 will discuss the prediction of the Indian monsoon onset. Section 6 will discuss the monthly forecast scores. Finally, Section 7 will discuss the main results.

2. Monthly Forecasting at ECMWF

Monthly forecasts are issued every Thursday at ECMWF. They consist of a 51-member ensemble (a control and 50 perturbed forecasts) integrated for 32 days. Since March 2008, the atmospheric model has a horizontal resolution is TL399 (about 60 kilometres) until day 10 and TL255 (about 80 kilometres) from day 10 to 32. The atmospheric vertical resolution has 62 vertical levels.

The atmospheric model is forced by persisted SST anomalies till day 10 and is coupled to an ocean general circulation model (OGCM) at day 10. The OGCM is HOPE from the Max Plank Institute (Wolff et al, 1997; Balmaseda et al 2004). The ocean initial conditions at day 10 are taken from the last day of a 10-day OGCM

integration, which is initialised from the ECMWF analysis (Balmaseda et al, 2008) and forced by the fluxes from the atmosphere-only integration.

The 50 perturbed forecasts are generated by perturbing both the atmosphere and ocean initial conditions. The atmospheric perturbations are the same as those applied to the medium-range ensemble forecasts: singular vectors to perturb the atmospheric initial conditions and stochastic perturbations during the model integrations. The oceanic initial conditions include a control and four perturbed ocean analyses: the perturbed ocean analyses are produced by adding randomly chosen patterns (computed by taking the difference between different wind analyses) to the wind forcing. Since the total ensemble size is 51, each of the 5 ocean assimilations is used as the initial condition of 10 or 11 (for the control assimilation) ensemble members.

Ideally, the atmospheric model should be coupled to the ocean model from days 0 to 32, but for technical reasons the T399 atmospheric and the ocean models cannot be coupled during the first 10 days. The initial conditions for the second leg of the forecast are produced by integrating the ocean alone forced by the atmospheric fluxes produced by each individual member during the first 10 days of atmosphere-only integrations. Future plans include coupling the atmosphere to the ocean model from day 0. More details about the ECMWF monthly forecasting system can be found in Vitart et al (2008).

3. Experimental framework

To investigate the role of upper ocean mixing and interactive SST on the monthly forecasts, a series of coupled ocean-atmosphere experiments has been performed. In all the experiments, the atmospheric component is the ECMWF atmospheric model Integrated Forecast System (IFS) run at T159 horizontal resolution (about 120 km resolution).

The first experiment uses the same ocean model as the ECMWF operational monthly forecasts after day 10. It is the Hamburg Ocean primitive Equation (HOPE) model (Wolff et al, 1997). The ocean model has a variable resolution going from about 0.3 degrees of latitude at the Equator to about 1.4 degrees in the extra-tropics by about 1.4 degrees in longitude everywhere. There are 29 vertical levels in the vertical with 10 meter resolution in the upper 100 m. The atmosphere and ocean are coupled using the OASIS coupler (Terray et al, 1995). Fluxes and SSTs are passed between the atmosphere and ocean every 1 hour. The atmospheric component is initialized the same way as the operational system, with atmospheric initial conditions taken from ERA40 (Uppala et al, 2005) and with perturbations to the initial conditions and stochastic physics active through the integration. The ocean initial conditions are taken from the ECMWF ocean analysis (Balmaseda et al, 2008). This experiment will be referred to as OGCM.

In the second experiment, the dynamical ocean model has been replaced by a 1D mixed layer model, with the same coupling technique as for the OGCM experiment. The mixed layer model is based on the KPP scheme (Large et al., 1994). It has a vertical domain of 200 m with 29 vertical levels. The vertical grid is stretched so that the top model level is 1.4 meter thick with 16 levels in the top 20 meters. The mixed layer model includes penetrative short wave radiation using the double exponential of (Paulson and Simpson 1977) for Jerlov water type IB (Jerlov, 1976). The horizontal resolution is the same as in the OGCM experiment. The mixed layer domain extends to +/- 44^o of latitude, poleward of which the SST is provided by persistence of the initial conditions. To produce a smooth transition between the fully coupled and uncoupled regions, the SST passed to the atmosphere between 40^o and 44^o is a weighted average of the modelled SST and the initial SST. No heat fluxes are applied to the mixed layer model to maintain its mean SST. The oceanic initial conditions are taken from the control member of the OGCM experiment (there are no oceanic perturbations in the ML experiment), linearly interpolated onto the mixed layer model vertical grid. This experiment will be referred to as ML.

4. Impact of ocean-atmosphere coupling on the prediction of the Madden-Julian Oscillation

In this section, both ML and OGCM have been integrated for 32 days each day from 15 December 1992 to 31 January 1993, during the Intense Observing Period of the Tropical Ocean Global Atmosphere Coupled Ocean-Atmosphere Response Experiment (TOGA COARE). The ensemble size is 5 (a control and 4 perturbed forecasts). The timing of the events is such that the initial conditions for the 48 5-member ensemble forecasts include all the phases of the MJO and each forecast lead time captures each phase of the MJO at least once.

To diagnose the MJO in the monthly forecasts, a combined EOF analysis of velocity potential at 200 hPa, outgoing longwave radiation (OLR) and zonal wind at 850 hPa anomalies (relative to the 1991-2003 climate) averaged between 10^o N and 10^o S has been performed on the ECMWF operational analysis from 1 January 2002 to 31 December 2004. This period, which is long enough to have a good representation of the intraseasonal variability, was chosen because of the lack of a strong ENSO event, which avoids the need to filter the interannual variability. The MJO diagnostics are similar to the method used in Wheeler and Hendon (2004), although Wheeler and Hendon (2004) used 200 hPa zonal wind rather than 200 hPa velocity potential.

The skill of the monthly forecasting system is then measured by performing a linear correlation between the observed time series of the Realtime Multivariate MJO series 1 (RMM1) and 2 (RMM2) with the forecast time series at different lead times. In the present paper we consider that the forecasts are skilful when the anomaly correlation is higher than 0.6.

Using this metrics, Woolnough et al (2007) found that ML produces significantly better forecasts of the MJO than OGCM, with IFS cycle 28r3 (Cy28r3). ML increases the skill of RMM1 by about 1 day and the skill of RMM2 by about 5 days. The largest improvement is for the principal component, which describes active convection over either the Indian Ocean or the West Pacific Warm Poll (RMM2). Woolnough et al (2007) attributed the better performance of ML to an improved representation of the diurnal cycle which results from the increased vertical resolution in the upper ocean. ML displays an enhanced sensitivity of the SSTs to the surface flux anomalies associated with the MJO.

The experiments described in Woolnough et al (2007) used a version of IFS, referred to as Cy28r3 which was operational in 2004 at ECMWF. Since 2004, several changes in the model physics have been introduced in IFS. To monitor their impact on the prediction of the MJO, the OGCM experiment has been repeated with the different operational cycles. Figure 1 shows how the representation of the Madden Julian Oscillation has evolved in IFS since 2004. In 2004, the amplitude of the Madden Julian Oscillation was too weak: the model lost more than 50% of the variance of velocity potential at 200 hPa after only a few days of integrations. However the propagation of the MJO was quite realistic. Since cycle 32r2 the amplitude of the MJO simulated by the model has improved. Cy32r3 is the first cycle able to maintain the amplitude of the MJO during the 32 days of integrations. However, the propagation of the MJO is not as realistic as it used to be, with the model having now difficulties propagating the MJO across the Maritime continent (Fig. 1).

A comparison between the performance of ML and OGCM has been performed with all the operational cycles. In all cases, ML produces better MJO forecasts than OGCM as in Woolnough et al (2007). However the amplitude of the improvement depends strongly on how good is the MJO propagation in the atmospheric model: with Cy30r2, ML extends by 6 days the skill of the model to predict the MJO (Fig. 2), whereas with Cy31r1 the improvement is of only 2 days. Cy30r2, which was not an operational cycle, produced the best scores for MJO propagation, whereas Cy31r1 is the cycle which displays the lowest MJO propagation scores since the monthly forecasting system became operational in 2004.

In summary, coupling IFS to an ocean mixed layer model rather to the OGCM which is currently used in the operational ECMWF monthly forecasting system produces significantly better predictions of the MJO. The amplitude of the improvement depends mostly on the skill of the atmospheric component to produce a realistic MJO in the first place. According to Woolnough et al (2007), the improvement obtained with ML is mostly due to the finer vertical resolution in the upper ocean, rather than to the mixing scheme.

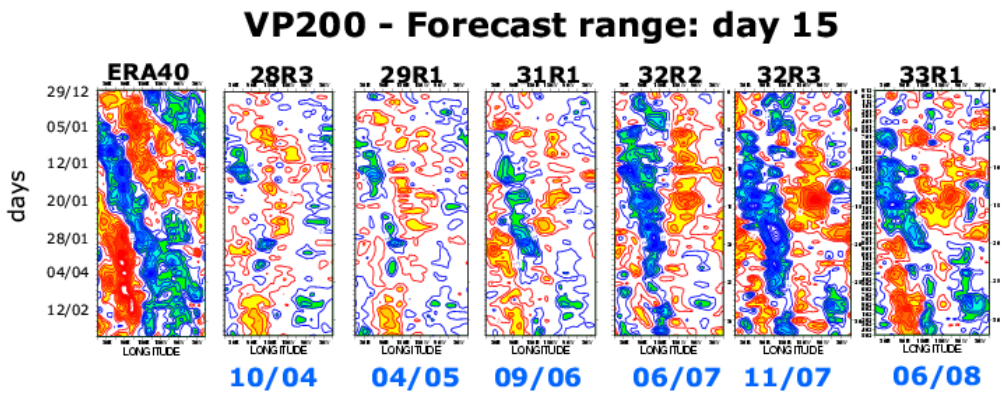

Figure 1: Hovmöller diagrams of the averaged outgoing long-wave radiation (OLR) between 10oS and 10oN from 29 December 1992 to 15 February 1993 as analyzed by ERA-40 and obtained from daily forecast with Cy28r3 to Cy32r3. Each forecast verifies at the 15-day lead time. Red shading denotes warm OLR anomalies (negative phase of the MJO) and blue shading cold anomalies (convective active phase of the MJO).

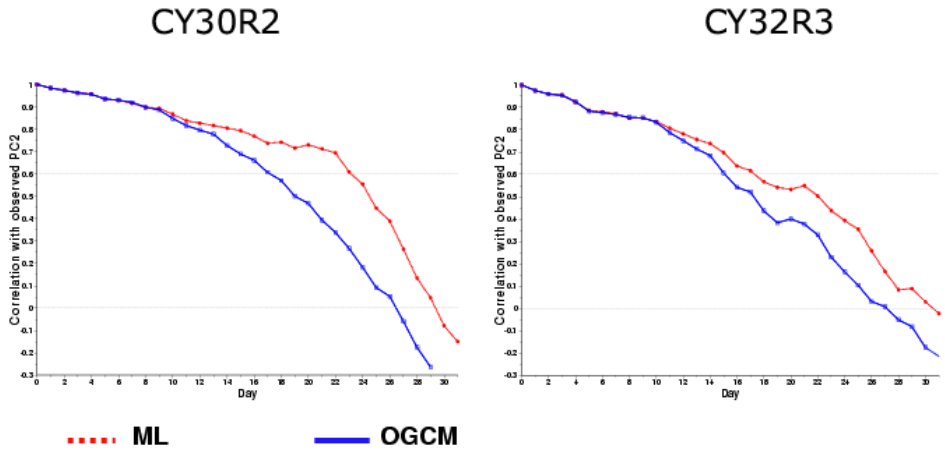

Figure 2: Correlation of the PC2 time series from ERA40 with the ensemble mean forecast time series, based on 48 start dates, for the OGCM experiment (solid blue line) and the ML experiment (solid red line). The left panel shows the correlations obtained with IFS Cycle 30R2, and the right panel shows the correlations obtained with Cycle 32R3.

5. Impact of ocean-atmosphere coupling on the prediction of the onset of the Indian monsoon

The prediction of Indian rainfall in June represents a particularly difficult challenge. During the month of June, the level of Indian rainfall is strongly linked to the onset of the monsoon, which is usually difficult to predict more than a couple of weeks in advance. The same experiments ML and OGCM as in Section 4 have been repeated to predict the Indian precipitation in June, but with a different setting: the model integrations start on 15 May 1991 to 2007 (18 years), and the model integrations have been extended to 46 days to cover the full month of June. The version of IFS used in this set of experiments is Cy31r2 which was operational from December 2006 until June 2007. The ensemble size has been extended to 15. More details about this experiment can be found in Vitart and Molteni (2008).

The interannual variability of precipitation over India (land only) has been computed for each experiment and averaged over the 15 members of the ensemble. After a few days of integrations, the model starts to drift towards its own climate. In this study the forecasts are calibrated using a cross-validation technique: for each experiment and for a given year, the model climate is computed by averaging all the ensemble forecasts of this experiment excluding the forecasts associated to this specific year. The model climate is then removed from the ensemble forecast to produce precipitation anomalies. The interannual variability of the ensemble mean precipitation anomalies over India is then compared to anomalies computed from Indian station data (Rajeevan et al, 2006).

ML produces better forecasts of the interannual variability of June precipitation over India (time range: day 16-45): the linear correlation between the ensemble mean variability from 1991 to 2007 and the station data time series is 0.62 for ML compared to 0.43 for OGCM. The RMS error is 0.84 for ML instead of 0.98 for MOFC. ML produced also better forecasts of Indian precipitation averaged in pentads (Fig. 3). MOFC displays some skill in predicting precipitation anomalies over India up to the 6-10 June pentad. ML on the other hand shows skill up to the 20-25 June pentad.

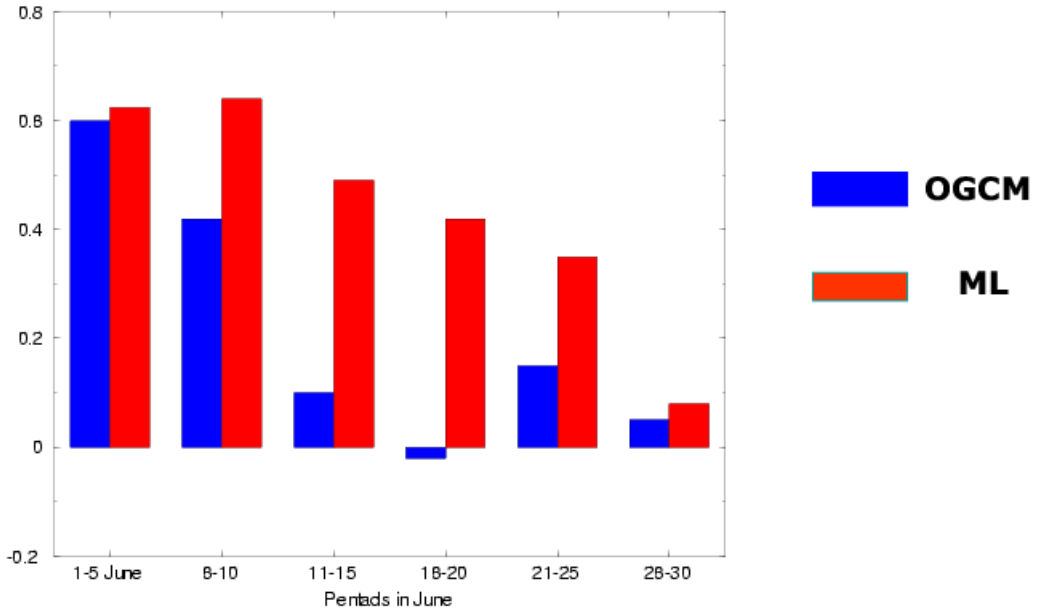

Figure 3: Linear correlation between the interannual variability of precipitation from Indian station data averaged over pentads in June from 1991 to 2007 and the ensemble mean precipitation predicted by OGCM (blue) and ML (red).

The better scores obtained with the ocean mixed layer model could be explained by a faster northward propagation of precipitation in ML than in MOFC (see example in Figure 4). Climatologically, during the first pentad in June, the South Kerala region receives a sudden burst of monsoon rainfall associated with the onset of the monsoon. The ML experiment is able to capture this maximum of climatological precipitation in the first pentad of June (day 16-20), although it may not be as sudden as in observations (Vitart and Molteni, 2008). On the other hand, MOFC has a maximum of precipitation about a week later. Those results suggest that the northward propagation of precipitation is more realistic in ML than in MOFC. This is likely to explain why the scores in ML are significantly higher than in MOFC, particularly for the prediction of pentads, where predicting the correct timing of the northward propagation of precipitation is crucial.

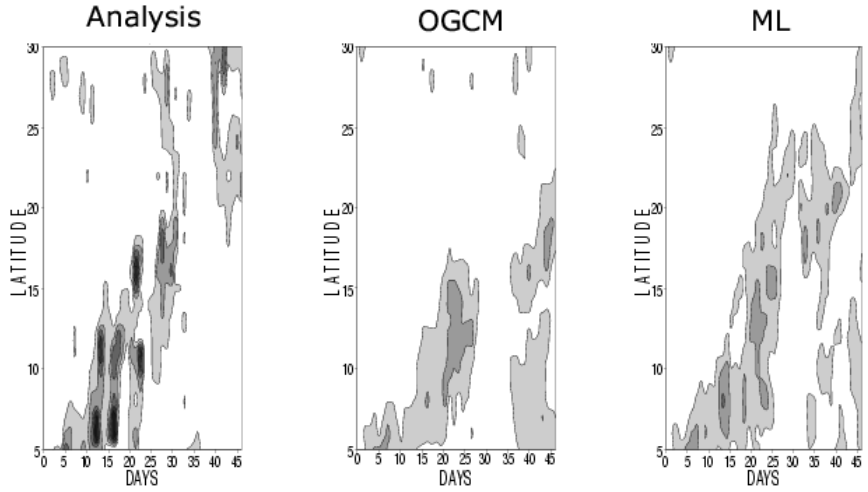

Figure 4: Hovmöller diagram of daily total precipitation anomalies (anomalies relative to the period 1991-2001) averaged between 70°E and 85°E in 1994. The y-axis represents the latitude between 5°N and 30°N. The x-axis represents the time range from 0 to 46 days, starting on 15 May. The left panel displays the analysis from ERA40, the middle panel displays the ensemble mean forecast from OGCM and the right panel displays the ensemble mean forecast from ML. The contour interval is 4 mm per day, with the first contour at 1 mm per day.

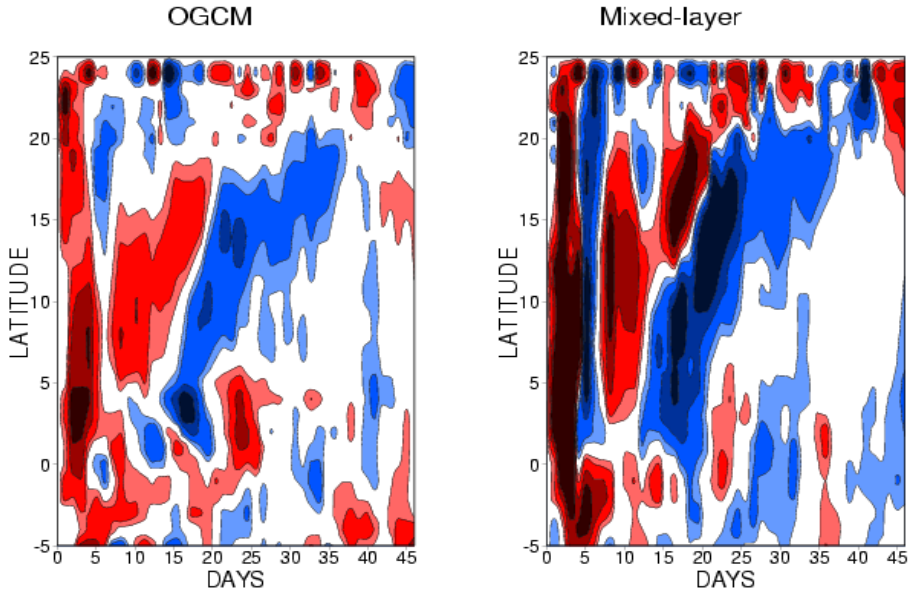

Figure 5: Hovmöller diagram of SST anomaly tendencies in 1994 (anomalies relative to the period 1991-2001) averaged between 60° E and 70° E for a) the ensemble mean of OGCM and b) the ensemble mean of ML. The tendencies have been computed by taking the difference between the SSTs at day n and day n^{-1}. The x-axis represents the time range from 0 to 46 days, starting on 15 May. The y-axis represents the latitude between 5° S and 30° N. The contour interval is 0.02° per day, with the first contour at 0.02o per day. Positive values are contoured.

The difference in the northward propagation between ML and MOFC could be explained by an enhanced sensitivity of the mixed layer model to the surface fluxes compared to the full dynamical ocean model. Figure 5 shows the time evolution of the tendencies of sea surface temperature in the Arabian Seas as a function of latitude. Both MOFC and ML display similar patterns with a warming preceding the northward propagation of precipitation, followed by a cooling of SSTs. However ML displays much stronger SST anomalies than MOFC. Woolnough et al (2007) found that the amplitude of SSTs in ML was much more realistic in ML than in MOFC. Therefore, MOFC is likely to underestimate the feed-back of the ocean on the northward propagation of precipitation. This may explain the more realistic monsoon precipitation forecasts in ML than in MOFC.

6. Impact of ocean-atmosphere coupling on monthly forecast scores.

Sections 4 and 5 have shown that a good representation of the mixing processes in the upper ocean benefits to the prediction of the MJO and the onset of the monsoon. This section will investigate if this is also the case for the monthly forecast scores.

The 46-day ML and OGCM experiments described in Section 5 have been repeated with a more recent IFS cycle (Cy32r3) and for the starting dates 15 May, 15 June and 15 July 1991-2007 to cover the months of June, July and August. Summer is a period which should be more favourable to OGCM, since it is the period when the SSTs associated to ENSO vary the fastest and when ML does not benefit from better MJO forecasts, since MJO events occur mostly in Winter and Spring.

Figure 6 shows the mean bias averaged over the period June, July and August and over the period 1991-2007 (time range day 16-45) for ML and OGCM. The biases in ML and OGCM display the same patterns and sign over most regions, except over the Indian Ocean, where ML has a cold bias and OGCM a warm bias. In most regions ML displays a lower bias than OGCM. However, the bias in ML is larger than in OGCM in the North East Pacific.

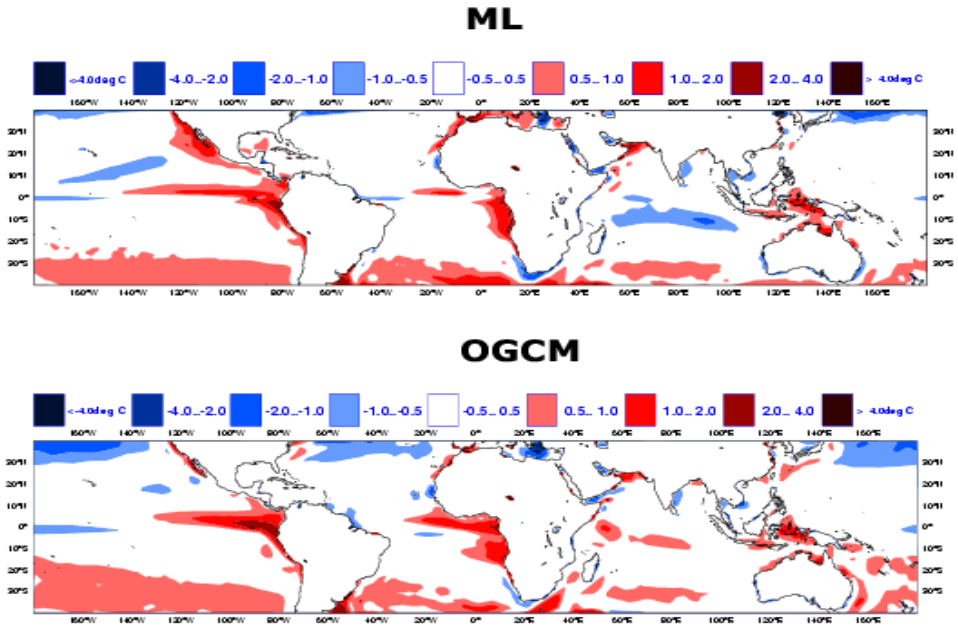

Figure 6: Mean SST bias for the period June-July-August between ML and Reynolds OIv2 (Reynolds et al, 2002) (top panel) and between OGCM and Reynolds OIv2 (bottom panel). The forecasts starting on 15 May, 15 June and 15 July have been averaged over the period day 16 to 45, over the 15 members of the ensemble and the period 1991-2007.

Figure 7 shows the linear correlation between the interannual variability of SST predicted by the coupled models and Reynolds OIv2 SSTs (Reynolds et al, 2001). The OGCM model displays higher skill in the eastern Pacific and tropical Indian Ocean than ML. On the other hand, ML is more skilful over the western North Pacifc and the subtropical North Atlantic. This is consistent with the skill of ML and OGCM to predict the interannual variability of the Accumulated Cyclone Energy (ACE) over the different ocean basins. ML and OGCM have comparable skill over the Atlantic, but ML outperforms OGCM over the western North Pacific, whereas OGCM outperforms ML in the eastern North Pacific (Table 1).

	ATL	ENP	WNP
OGCM	0.72	0.63	0.47
ML	0.74	0.50	0.60

Table 1: Linear correlation between the August mean accumulated cyclone energy (ACE) predicted by ML and OGCM starting on 15 July (time range day 16-45) 1978-2007 and observations from HURDAT (http://www.aoml.noaa.gov/hrd/hurdat) for 3 different basins. The basins are: the North Atlantic (ATL), the eastern North Pacific (ENP) and the western North Pacific (WNP).

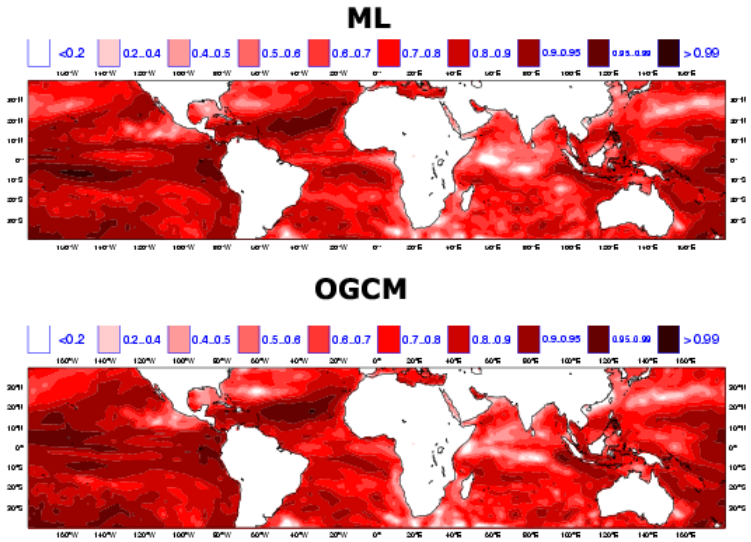

Figure 7: Linear correlation between the ensemble mean of ML and Reynolds OIv2 (top panel) and the ensemble mean of OGCM and Reynolds OIv2 (bottom panel). The linear correlation has been averaged over the period June-July-August for the forecasts starting on 15 May, 15 June and 15 July. The time range of the forecast is day 16-45.

In order to evaluate the impact of the ocean-atmosphere coupling on the monthly forecast scores, the ROC scores (Stanski et al, 1989) of temperature at 850 hPA (T850) have been computed over all the cases in June, July August for the period day 16-45 for ML and OGCM. ML and OGCM show overall similar patterns of skill for this time range (Fig.8a and b), but OGCM displays better scores over East Africa, South Africa and Central South America than ML, which is consistent with better SST predictions over the tropical Indian and eastern Pacific (Fig. 8c). On the other hand, the ROC areas are generally higher in the Northern Extratropics with ML than OGCM. A similar conclusion is obtained when using the Brier Skill score (Brier, 1950) and with precipitation. Scatter plot diagrams of ROC and BSS scores indicate that ML is in general more skilful than OGCM to predict T850 and precipitation over the Northern Extratropics (not shown). The difference is however not statistically significant within the 10% level of confidence. However, the difference is statistically significant at the 5% level of confidence for both precipitation and T850, and ROC and BSS scores in the second half of this period (day 31-45). Future plans include investigating if this result is valid for the other seasons.

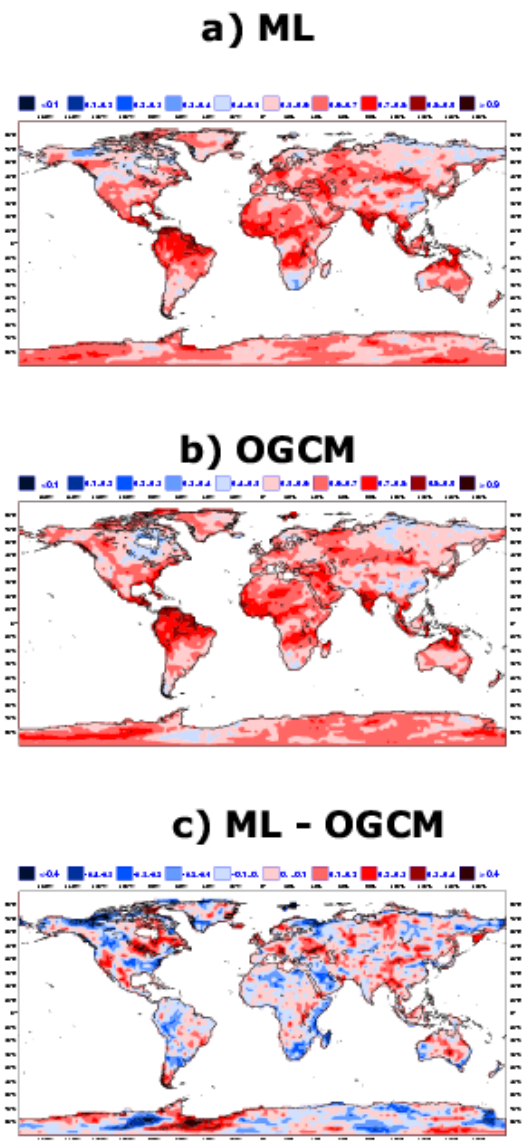

Figure 8: ROC area of the probability that the monthly mean temperature at 850 hPa in June, July and August 1991 to 2007 is in the upper tercile for a) ML and b) OGCM. In a) and b), the red contours indicate a ROC area larger than 0.5, and the blue contours indicate a ROC area less than 0.5. Panel c) shows the difference of ROC area between ML and OGCM. In panel c), the red contours indicate areas where ML outperforms OGCM. Blue contours indicate areas where OGCM outperforms ML.

7. Conclusion

The main conclusion of this paper is that the ocean mixed layer processes are important for monthly forecasting. Their impact on the monthly forecasts is not small: the skill to predict the MJO can be improved by up to 6 days and the skill to predict Indian monsoon rainfall can be increased by 2 to 3 pentads with a good representation of the ocean mixed layer processes. The prediction of T850 and precipitation in the northern Extratropics is also improved in summer when using an ocean mixed layer model. Therefore the ocean mixed layer processes seem to play a more important role than ocean dynamics at this time range.

Those results suggest that the current configuration of the monthly forecasting system at ECMWF is not optimal and that there is room for a significant improvement in the ECMWF monthly forecasts. The OGCM used in the current monthly forecasts has a configuration which has not been designed for monthly forecasting, but for seasonal forecasting (most especially for ENSO prediction) and suffers from a particularly low vertical resolution in the upper ocean.

An ocean mixed layer model could be an alternative to an OGCM for this time range. Work is in progress at ECMWF to implement the KPP scheme as a subroutine in IFS. This will allow the testing of coupled integrations at very high horizontal resolution.

Some questions still need to be addressed, like the impact of horizontal resolution for monthly forecasts, the behaviour of the mixed layer model at high latitudes and which configuration to adopt for seamless prediction. It is possible that a variable ocean resolution would be needed for a seamless system covering medium-range, monthly and seasonal forecasts.

8. References

Anderson, D., T. Stockdale, M. Balmaseda, L. Ferranti, F. Vitart, F. Molteni, F. Doblas-Reyes, K. Mogensen and A. Vidard, 2007: Seasonal Forecasting System 3. *ECMWF Technical Memo*, No.503.

Balmaseda, M.A., 2004: Ocean data assimilation for seasonal forecasts. ECMWF Seminar Proceedings. *Seminar on Recent developments in data assimilation for atmosphere and ocean*, 8-12 September 2003, 301-326.

Balmaseda, M.A., A. Vidard, and D.L.T. Anderson, 2008: The ECMWF Ocean Analysis System: ORA-S3. *Mon. Wea. Rev.*, **136**, 3018-3034.

Brier, G. W., 1950: Verification of forecasts expressed in terms of probabilities. *Mon. Wea. Rev.*, **78**, 1-3.

Jerlov, N.G., 1976: *Marine Optics*, Elsevier: New York.

Large, W.G., J. C. Mc Williams, S. C. Doney, 1994: Oceanic vertical mixing: A review and a model with a nonlocal boundary layer parameterization. *Rev. Geophys.,* **32**, 363-403.

Paulson CA, J. J. Simpson, 1977: Irradiance Measurements in the Upper Ocean. *J. phys. Oceanogr.,* **7**: 952-956.

Rajeevan, M., J. Bhate, J.D. Kale, and B. Lal, 2006: High resolution daily gridded rainfall data for the Indian Region: Analysis of break and active monsoon spells. *Current Science,* **91**, 3, 296-306.

Reynolds, R. W., N.A. Rayner, T. M. Smith, D. C. Stokes, and W. Wang, 2002: An improved in situ and satellite SST analysis for climate. *J. Climate*, **15**, 1609-1625.

Stanski, H. R., L. J. Wilson, and W. R. Burrows, 1989: Survey of common verification methods in meteorology. *World Weather Watch Tech. Rep.* 8, WMO Tech. Doc. 358, 114 pp.

Terray, L., E. Sevault, E. Guilyard and O. Thual, 1995L. The OASIS coupler user guide version 2.0. *CERFACS Technical report*, TR-CMGC 95-46.

Uppala, S. and Co-authors, 2005: The ERA-40 reanalysis. *Quart. J. Roy. Meteor. Soc.*, **131**, 2961-3012.

Vitart, F., R. Buizza, M. Alonso Balmaseda, G. Balsamo, J.-R. Bidlot, A. Bonet, M. Fuentes, A. Hofstadler, F. Moleni and T. Palmer: The new VAREPS-monthly forecasting system: a first step towards seamless prediction. *Quart. J. Roy. Meteor. Soc.,* in press.

Vitart, F. and F. Molteni, 2008: Dynamical extended-range prediction of early monsoon rainfall over India. *Mon. Wea. Rev,* in press.

Wheeler, M.C., and H. H. Hendon, 2004: An all-season real-time multivariate MJO index: Development of an index for monitoring and prediction. *Mon. Wea. Rev,*. **132**, 1917-1932.

Wolff, J.O., E.Maier-Raimer, and S. Legutke, 1997: The Hamburg ocean primitive equation model. *Deutsches Klimarechenzentrum Tech. Rep.* 13, Hamburg, Germany, 98 pp.

Woolnough, S.J., F. Vitart and M.A. Balmaseda, 2007: The role of the ocean in the Madden-Julian Oscillation: Implications for MJO prediction. *Q. J. R. Meteorol. Soc.*, **133**, 117-128.